Active Galactic Nuclei Shed Light on Axionlike Particles

Clare Burrage,[1] Anne-Christine Davis,[2] and Douglas J. Shaw[3]

[1]*Theory Group, Deutsches Elektronen-Synchrotron DESY, D-22603 Hamburg, Germany*
[2]*Department of Applied Mathematics and Theoretical Physics, Centre for Mathematical Sciences, Cambridge CB3 0WA, United Kingdom*
[3]*Queen Mary University of London, Astronomy Unit, School of Mathematical Sciences, Mile End Road, London E1 4NS, United Kingdom*

(Received 17 February 2009; revised manuscript received 25 March 2009; published 21 May 2009)

We demonstrate that the scatter in the luminosity relations of astrophysical objects can be used to search for axionlike particles. This analysis is applied to observations of active galactic nuclei, where we find evidence highly suggestive of the existence of a very light axionlike particle.

DOI: 10.1103/PhysRevLett.102.201101 PACS numbers: 98.54.Cm, 14.80.Mz

Precision observations of the recent Universe are an invaluable test bed for ''new physics'' such as the existence of new, low mass and/or weakly interacting particles. Such a particle, the axion, was proposed in 1977 by Pecci and Quinn to solve the strong *CP* problem [1]. Since then, other models which also feature (very) light, neutral spin zero, axionlike particles (ALPs) have been proposed, e.g., [2,3]. Recently, analyses of starlight polarization [4] and the properties of high energy cosmic rays [5] have provided tentative evidence for ALPs.

In this Letter, we present a new method for studying ALPs using astrophysical x- or γ-ray luminosity relations, which, when applied to observations of active galactic nuclei (AGN), provides the strongest evidence yet for the existence of ALPs.

ALPs are scalar or pseudoscalar particles, ϕ, which couple to photons, A^μ, via the terms $(\phi/M)F_{\mu\nu}F^{\mu\nu}$ or $(\phi/M)\epsilon_{\mu\nu\rho\sigma}F^{\mu\nu}F^{\rho\sigma}$ in the Lagrangian, respectively; $F_{\mu\nu} = 2\partial_{[\mu}A_{\nu]}$. We define m_ϕ to be the ALP mass, and $g_{\gamma\gamma\phi} = 1/M$ is the coupling between ALPs and photons.

In the presence of a background magnetic field B, ALPs mix with photons. The probability that an ALP converts into a photon while traveling through a coherent magnetic domain of length l is [6]

$$P_{\gamma\leftrightarrow\phi} = \sin^2 2\theta \sin^2\left(\frac{\Delta}{\cos 2\theta}\right), \tag{1}$$

where $\Delta = m_{\rm eff}^2 l/4\omega$, $\tan 2\theta = 2B\omega/Mm_{\rm eff}^2$, $m_{\rm eff}^2 = m_\phi^2 - \omega_{\rm pl}^2 - \epsilon B^2/M^2$; $\hbar, c = 1$. $\omega_{\rm pl}^2 = 4\pi\alpha_{\rm em} n_e/m_e$ is the plasma frequency; n_e is the electron number density, m_e the electron mass, and $\alpha_{\rm em} \approx 1/137$ is the electromagnetic fine structure constant. $\epsilon = +1$ for scalars and 0 for pseudoscalars; generally, $B^2/M^2\|m_\phi - \omega_{\rm pl}^2\| \ll 1$. The total flux (in ALPs and photons) is conserved by the mixing process; however, the photon number is not.

ALP-photon mixing is constrained by a number of laboratory experiments (see Ref. [3] and references therein), but the tightest constraints come from the astrophysical consequences of ALPs (see Ref. [7]).

We are concerned with very light ALPs, $m_\phi \ll 10^{-12}$ eV. For such masses, observations of the supernova SN 1987A limit $g_{11} = 10^{11}\ {\rm GeV}/M \lesssim 1$ [3] for pseudoscalars, while limits on new long range forces require $g_{11} < 10^{-16}$ for scalars. However, if ALPs are chameleonic, these constraints do not apply [2,4], and the best constraint comes from the structure of starlight polarization: $g_{11} \lesssim 100$ [4].

As photon number is not conserved, ALP-photon mixing in astrophysical magnetic fields alters the observed luminosity of objects. In this Letter, we consider light that has traveled through $N \gg 1$ randomly oriented magnetic regions. This is true of light from many astrophysical sources, particularly those in galaxy clusters. We focus on the limit in which the mixing is strong, $NP_{\gamma\leftrightarrow\phi} \gg 1$, and frequency independent, $N\Delta \lesssim \pi/2$.

In this strong mixing limit, little or no circular polarization is produced [4] and power is spread with equal probability between the two photon polarization states, γ_1 and γ_2, and the ALP, ϕ. We take $I^{({\rm tot})1/2}\mathbf{u} = (\gamma_1, \gamma_2, \phi)^T$ to be real. Since $\|\mathbf{u}\|^2 = 1$ is conserved, $\mathbf{u}$ describes a point on a sphere, and any point is as likely as any other. Thus, after strong mixing, the normalized final state $\mathbf{u}$ is a random vector:

$$\mathbf{u} = (\sqrt{1-K^2}\cos\pi\Theta, \sqrt{1-K^2}\sin\pi\Theta, K)^T,$$

where $K, \Theta \sim U(-1, 1)$, and the final flux in the photon field is $I_f^{(\gamma)} = (1-K^2)I^{({\rm tot})}$. The initial photon flux is $I_0^{(\gamma)}$ and we assume $I_0^{(\gamma)} \approx I^{({\rm tot})}$. A state labeled by a real vector $\mathbf{u}$ is sufficient to describe any mixture of ϕ with fully linearly polarized light. We extend this result to light with partial or no initial linear polarization by noting that any such state, with $I_0^{(\gamma)} \approx I^{({\rm tot})}$, can be written as a superposition of two real $\mathbf{u}$ state vectors [4]. Where p_0 is the initial degree of net linear polarization, the final photon flux after strong mixing is

$$I_f^{(\gamma)} = [1 - (1 + p_0)K_1^2/2 - (1 - p_0)K_2^2/2]I^{(\mathrm{tot})}, \quad (2)$$

where $K_i \sim U(-1, 1)$. We define $C \equiv I_f^{(\gamma)}/I^{(\mathrm{tot})}$. Averaging C over many different light paths through a large number of randomly oriented magnetic regions gives $\bar{C} = 2/3$. This average reduction in the apparent luminosity of astrophysical sources is well known [8]; however, attempts to use it to constrain ALPs have, so far, been unsuccessful since the intrinsic luminosity of the astrophysical objects is not known with sufficient accuracy. It is rarely appreciated that $C = 2/3$ only when averaged over many different light paths (e.g., light from many different objects). For a given light path through the magnetic regions, there is significant scatter and skew of C about its mean of $2/3$ [4]. From Eq. (2), the probability that $C \in [c, c + dc]$ is $f_C(c; p_0)dc$, where

$$f_C(c; p_0) = \frac{1}{\sqrt{1 - p_0^2}}\left\{\tan^{-1}\left[\sqrt{a}\left(1 - \frac{2c_+}{1 + p_0}\right)^{-1/2}\right] - \tan^{-1}\left[\sqrt{a}\left(1 - \frac{2c_-}{1 - p_0}\right)^{1/2}\right]\right\}, \quad (3)$$

and $a = (1 - p_0)/(1 + p_0)$; $c_\pm = \min(c, (1 \pm p_0)/2)$.

The central idea of this Letter is that the scatter in empirically established luminosity relations can constrain or rule out strong mixing between ALPs and photons. Provided ω is high enough, strong and (almost) frequency independent mixing can be caused by the magnetic fields of galaxy clusters [4], the existence of which is well established [9]. When such mixing occurs, there will be a contribution to the scatter of the observed luminosities as described by Eq. (3). Observations imply that most clusters contain magnetic fields of strength $B \approx 1$–10 μG which are generally coherent over $l \sim 1$–100 kpc scales; typically, $Bl^{1/2} \sim (5$–$10)$ $\mu\mathrm{G}(10\ \mathrm{kpc})^{1/2}$ [9]. Typical electron densities in the diffuse plasma in the intracluster medium (ICM) are $n_e \sim 10^{-3}\ \mathrm{cm}^{-3}$ and hence $\omega_{\mathrm{pl}} \sim 10^{-12}$ eV, and we require $m_\phi^2 \lesssim \omega_{\mathrm{pl}}^2$.

If light travels a typical distance of $L = 0.1$–1 Mpc through the ICM, then $N = L/l \gg 1$ magnetic domains will have been traversed. Strong mixing requires $N \gg 1$ and $NP_{\gamma\leftrightarrow\phi} \gg 1$, so $(B\sqrt{lL}/2M)^2 \gg 1$ and $\sqrt{N}2B\omega/M\omega_{\mathrm{pl}}^2 \gg 1$. With $B_8 = B/8$ μG, $l_{10} = L/10$ kpc, $L_{200} = L/200$ kpc, and $g_{11} = 10^{11}\ \mathrm{GeV}/M$, we have $(B/2M)^2 lL \approx 30.0 g_{11}^2 B_8^2 l_{10} L_{200}$. Typically $B_8^2 l_{10} L_{200} \sim \mathcal{O}(1)$ and for $N \sim 30$–1000 we need $\omega \gg$ 16–170 eV. Frequency independent mixing, $N\Delta \lesssim \pi/2$, i.e., requires $\omega \gtrsim \omega_{\mathrm{pl}}^2 L/2\pi = 3$–$30$ keV. Numerical simulations show that the frequency independent limit is still approximately valid for frequencies that are a factor of 10 smaller; i.e., $\omega \gtrsim 0.3$–3 keV. When $NP_{\gamma\leftrightarrow\phi} \gg 1$, $N\Delta \gg 1$ the measured luminosity is attenuated by a factor of $2/3$ with relatively little scatter.

For the remainder of this Letter, we assume that $\omega \gtrsim$ 2 keV light, i.e., x rays or γ rays, which originated in or passed through a galaxy cluster, has undergone strong and (almost) frequency independent ALP mixing, requiring $g_{11} \gtrsim 0.1$–0.3 and $m_\phi \lesssim 10^{-12}$ eV. This is allowed for pseudoscalar and chameleonic ALPs. For $\omega \ll 0.5$ keV, mixing is highly frequency dependent and can be either weak (so $C \approx 1$) or strong. In the latter case the luminosity is reduced by a factor $\approx 2/3$.

We require that the x- or γ-ray sources are compact; i.e., their size R is $\lesssim L \sim$ few kpc. Diffuse light, such as the x-ray light from galaxy clusters ($R \sim 10^2$–10^3 kpc) is not suitable for our analysis as it will have traced many different paths through the magnetic fields of the cluster, and the effects of mixing will be averaged over all of these paths. For such sources, the main effect of strong mixing is the $2/3$ suppression of the total luminosity.

For a number of classes of compact astrophysical objects, correlations between the x- or γ-ray luminosity or radiated energy and some feature of their light curve (e.g., peak energy) or the object's luminosity at a lower frequency have been empirically established. We let Y_i label the x- or γ-ray luminosity or total energy and X_i label the light-curve feature or lower energy luminosity with which it is correlated. The relations between Y_i and X_i take the form

$$\log_{10} Y_i = a + b\log_{10} X_i + S_i, \quad (4)$$

where S_i vanish on average, and represent the scatter of individual measurements about the mean relation. The scatter comes partly from measurement error, but in most cases the largest contribution appears to be intrinsic (e.g., [10]). It is standard practice to model the S_i as being normally distributed with mean 0 and some variance σ^2. i.e.. $S_i = \sigma\delta_i$, where $\delta_i \sim N(0, 1)$. We refer to this as the Gaussian scatter model. If the high frequency light has been subject to strong mixing with an ALP, we expect

$$S_i = \sigma\delta_i - \log_{10} C_i + \mu, \quad (5)$$

and C_i has probability density function $f_C(c)$ as given above. μ is the expectation of $\log_{10} C_i$, so the S_i still have mean 0; μ can always be absorbed into a redefinition of the fitting parameter a. We call this the ALP strong mixing (ALPSM) scatter model. The distribution of the $\log_{10} C_i$ is both a distinct feature of strong mixing and very different from a normal distribution. Provided the variance of the intrinsic Gaussian scatter (σ^2 in both models) is not too large, it is possible, with enough measurements, to use the distribution of the scatter to constrain, detect, or rule out such strong mixing. We do this by means of a likelihood ratio test, comparing the null Gaussian hypothesis with the ALPSM hypothesis. Both models have the form $S_i = \sigma\delta_i + \log_{10}((1 - f) + fC_i)$; f parametrizes the fraction of light that is strongly mixed. $0 < f < 1$ corresponds to partial strong mixing. However, along a given path, either strong mixing occurs or it does not; the x- or γ-ray light from an object cannot be partially strongly mixed. f is not therefore a free parameter to be fitted. The likelihood

L_f of the model with general f is

$$L_f(a, b, \sigma; p_0) = \prod_i \frac{1}{\sqrt{2\pi}\sigma} \int_0^1 e^{-(z_i^2/2\sigma^2)} f_C(c; p_0) dc, \quad (6)$$

where $z_i = \log_{10} Y_i - a - b \log_{10} X_i - h(c; f)$ and $h(c; f) = \log_{10}((1-f) + fc)$. We find $\{a, b, \sigma\} = \{\hat{a}, \hat{b}, \hat{\sigma}\}$, which maximize L_f. We define $\hat{L}_f(p_0) = L_f(\hat{a}, \hat{b}, \hat{\sigma}; p_0)$ and

$$r_f(p_0) = 2 \ln(\hat{L}_f(p_0)/\hat{L}_0).$$

Keeping p_0 fixed, both the Gaussian and ALPSM models have the same number of free parameters. This means that $r_1(p_0)$ is equivalent to the Bayesian information criteria commonly used for model selection. Conventionally, $r_1(p_0) < -6 (r_0 > 6)$ would be "strong evidence" against (for) the ALP strong mixing model over the Gaussian one. $\|r_1\| > 10$ corresponds to "very strong evidence." If ALPs are preferred, a useful check is to ensure that $r_f(p_0)$ is maximized for $f \approx 1$. If this is not the case, we would conclude that while the data are not compatible with simple Gaussian scatter, it is also not particularly indicative of the strong mixing with ALPs.

Luminosity relations of the required form exist for gamma ray bursts (GRBs) [10], blazars [11,12], and AGN [13], and are suitable for our analysis. An $\mathcal{O}(1)$ fraction of such objects are expected to be in galaxy clusters.

The γ-ray luminosity L_γ and radiated energy E_γ of GRBs have been found to be correlated with a number of spectral features, giving five seemingly independent relations (see [10]). Additionally the L_γ of blazars, a class of AGN, is correlated with both their radio wave L_r [11] and near infrared [12] luminosities L_k. We analyzed observations of 69 GRBs [10], with redshifts $z = 0.17$–6.6, 95 EGRET observations of blazars with $z \approx 0.02$–2.5 [11] for the radio relation, and 16 blazars ($z \approx 0.3$–1) for the IR relation [12]. For all the relations, however, either data points were too few or the intrinsic Gaussian scatter was too large to constrain ALP mixing. For four out of five GRB relations and both blazar relations, $r_1 > 0$, but in all cases $|r_1| < 0.75$; the sum of these r_1's is only $r_1 \approx 1.6$ for $p_0 = 0$ (with similar values for other p_0) a statistically insignificant preference for the ALPSM model.

There is also a strong correlation between the 2 keV monochromatic x-ray luminosity, L_X, of AGN and their monochromatic optical luminosity L_o (at 2500 Å; $\omega \approx 4.95$ eV) [13]. This relation is of the form $\log L_X \approx a + b \log L_o$. We use observations of 77 optically selected AGNs with $z = 0.061$–2.54 from the COMBO-17 and ROSAT surveys as tabulated in Ref. [13] to analyze the scatter in this relationship. For $0 \leq p_0 \lesssim 0.4$, we find

$$r_1(p_0)^{\mathrm{AGN}} \approx 14, \quad (7)$$

and for all p_0, $r_1(p_0)^{\mathrm{AGN}} > 11$. The weak dependence on p_0 means that the preference for ALPSM over the Gaussian model is robust to relaxing the universality of p_0 and including a marginalization over different prior distributions for p_0. For AGN, typically $p_0 \lesssim \mathcal{O}(10\%)$ at 2 keV [14]. Additionally, $r_f(p_0)$ is strongly peaked at $f = 1$: $r_1(0) \approx 14.1$ and $r_{0.9}(0) \approx 4.9$. We define P_{mix} to be the probability that light from a given object passes through a magnetic region where strong mixing occurs. In the ALPSM above we have taken $P_{\mathrm{mix}} = 1$. Our result is, however, robust to different values of P_{mix} with the current data only giving the weak constraint: $P_{\mathrm{mix}} \geq 0.08$ at 95% confidence. This is entirely consistent with the $\mathcal{O}(1)$ value we expect for mixing in the ICM.

There is clearly a structure in the scatter fitted better by ALP mixing than by the Gaussian scatter model. It is not clear, however, whether this is due to the success of the former or the failure of the latter which was only adopted for convenience, and because for other relations (e.g., those of GRB or Blazars), it provides a good fit to the scatter. It may be that if AGN physics were better understood, a non-Gaussian null hypothesis for the scatter distribution would be predicted that is a better fit than the ALP mixing model. While we cannot rule out this scenario, we can, independent of any null hypothesis, qualitatively check whether the structure of the scatter is actually well matched by the ALP mixing model.

We perform such a check by making 10^5 bootstrap resamplings with replacement, $D^* = \langle x_i^*, y_i^* \rangle$, of the original data, $D = \langle x_i \equiv \log_{10} X_i, y_i \equiv \log_{10} Y_i \rangle$. Both D and the D^* have $N_p = 77$ data points. For each D^* we match the relation $s_i^* = y_i^* - (a^* + b^* x_i^*)$; $\bar{s}^* \equiv k_1 = 0$ by minimizing the $\sigma_{\mathrm{rms}} \equiv k_2$, where

$$k_m(\{s_i\}) = \left(N_p^{-1} \sum_i s_i^{*m} \right)^{1/m}. \quad (8)$$

k_2 is the rms average of the s_i and k_3^3/k_2^3 is their skewness. Two-dimensional histograms of k_i vs k_j reveal nontrivial correlations between the k_m and, unlike the likelihood analysis, are relatively insensitive to any outlying data points. For comparison, we simulate data sets for both the best-fit Gaussian and ALPSM models in which $\hat{\sigma} = 0.34$ and $\hat{\sigma} = 0.23$, respectively, and ensure $\sigma_{\mathrm{rms}} \approx 0.34$ for each simulation. We plot the resampled $\{k_2, k_3\}$.

The detailed form of the plots varies from simulation to simulation; however, a number of qualitative features can be identified as "fingerprints" of the Gaussian or ALPSM models. In the former, there are two density peaks around $\{k_2, k_3\} \approx \{0.34, \pm 0.25\}$, whereas in the latter similar peaks often occur around $\approx \{0.23 - 0.3, \pm 0.15\}$. The main fingerprint of the best-fit ALPSM model, which occurs in most, if not all, of the simulations, is that most of the data points fall in a long "tail" $\{k_2, k_3\} \sim \{0.3, -0.3\}$ to $\{(0.4 - 0.5), -(0.5 - 0.7)\}$. These features persist for different values and distributions of $p_0 \lesssim 0.5$, and in more realistic simulations where $P_{\mathrm{mix}} < 100\%$. These features can be clearly seen in Figs. 1(a) and 1(b) which are, respectively, typical $k_2 - k_3$ histograms for data sets simu-

lated with the best-fit Gaussian and ALPSM models. Darker regions indicate higher density.

Figure 1(c) is the $k_2 - k_3$ plot for the actual AGN data. There is a marked qualitative similarity between Fig. 1(c) and the sample ALPSM model plot, Fig. 1(b). A dense tail-like feature is clearly present and its extent, direction, and structure of peaks are typical of that seen in the ALP simulations. Although not shown here, there is also a strong similarity between the AGN $k_3 - k_5$ plot and those found in the best-fit ALPSM model simulations. It should be noted that the data sets used have a potential observational bias *away* from the ALP model. The ALPSM predicts a $\log L_X$ distribution with a negative skew. All AGN in the data set had L_o observations but some only had an upper bound on L_X; such objects were excluded potentially correcting slightly the negative skew induced by strong mixing. No evidence for any correlation between redshift and scatter was found, ruling out an explanation for it based on evolution of the $L_X - L_o$ relation and/or an inaccurate choice of cosmological model. In the ALPSM model, additional scatter is induced in L_X. We cannot, however, say whether the unusual scatter in AGN data is due to scatter in L_X (as predicted by the ALPSM model) or in L_o. In principle, this degeneracy could be lifted if there were correlation between L_o for the AGN used here and some other low energy quantity unaffected by ALP mixing with sufficiently low scatter. At present we are unaware of any relevant observations. The proposed International X-ray Observatory (IXO) could verify or rule out the ALPSM model by measuring the x-ray polarization of AGN [4]. Nonchameleonic ALPs with the required properties could potentially be detected by the Cern Axion Solar Telescope (CAST). Ongoing efforts to constrain photon-ALP conversion in the Galactic magnetic field [4,5] probe similar ALP masses and couplings to those required for strong mixing. The effect searched for by Fairbairn *et al.* in Ref. [5] requires strong photon-ALP mixing in AGN magnetic fields; such mixing, if it occurs, could also explain the AGN $L_X - L_o$ scatter.

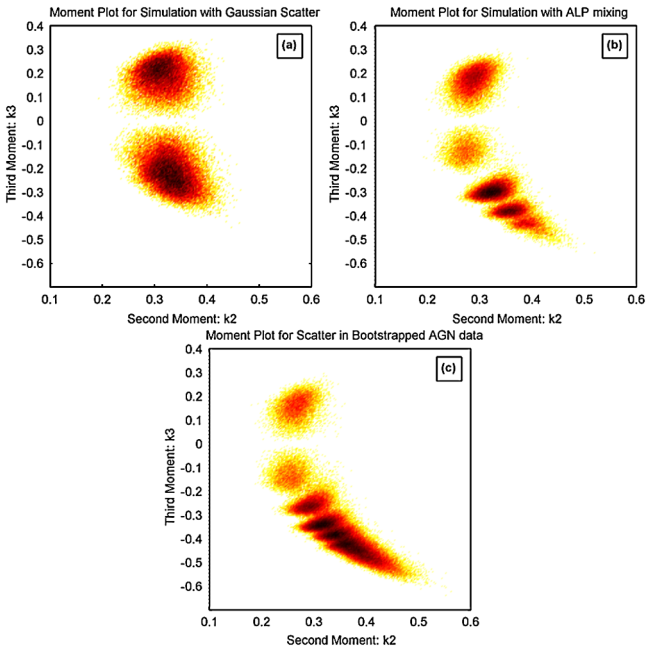

FIG. 1 (color online). Histograms of second (k_2) and third (k_3) moments [see Eq. (8)] for 10^5 resamplings of 77 data points (a) simulated with the best-fit Gaussian scatter ($\sigma = 0.34$), (b) simulated with the best-fit ALP mixing model ($\sigma = 0.23$), and (c) from the observed scatter in the AGN $L_X - L_o$ relation. Darker regions indicate higher density. See text for discussion.

In this Letter, we have shown that the scatter in empirical x- or γ-ray luminosity relations can be used to constrain mixing between ALPs and photons. When applied to the AGN $L_X - L_o$ relation, this shows strong evidence for ALPs relative to the null hypothesis of Gaussian scatter. Additionally, the visualizations of the AGN data reveal a scatter distribution with a strong qualitative similarity to that predicted by the best-fit ALP-photon strong mixing model. This similarity is independent of the null hypothesis. Strong mixing of ALPs with keV photons will occur in galaxy clusters if $M \lesssim \text{few} \times 10^{11}$ GeV and $m_\phi \ll 10^{-12}$ eV, or possibly in magnetic fields close to the AGN if $M \sim 10^{10}$ GeV and $m_\phi \ll 10^{-7}$ eV. While we cannot rule out explanations of the scatter in terms of known physics, it is, at the very least, a remarkable coincidence that both this and other recent analyses [4,5] are fitted better by models in which very light ALPs (with similar couplings and masses) exist.

C. B. acknowledges the German Science Foundation (DFG) under the Collaborative Research Centre (SFB) 676. A. C. D. and D. J. S. acknowledge STFC.

[1] R. D. Peccei and H. R. Quinn, Phys. Rev. Lett. **38**, 1440 (1977); Phys. Rev. D **16**, 1791 (1977).
[2] A. A. Anselm and N. G. Uraltsev, Phys. Lett. B **114**, 39 (1982); P. Svrcek and E. Witten, J. High Energy Phys. 06 (2006) 051; Ph. Brax, C. van de Bruck, and A. C. Davis, Phys. Rev. Lett. **99**, 121103 (2007).
[3] C. Amsler *et al.* (Particle Data Group), Phys. Lett. B **667**, 1 (2008).
[4] C. Burrage, A. C. Davis, and D. J. Shaw, Phys. Rev. D **79**, 044028 (2009).
[5] M. Fairbairn, T. Rashba, and S. Troitsky, arXiv:0901.4085; M. Roncadelli, A. De Angelis, and O. Mansutti, AIP Conf. Proc. **1018**, 147 (2008).
[6] G. Raffelt and L. Stodolsky, Phys. Rev. D **37**, 1237 (1988).
[7] G. G. Raffelt, Lect. Notes Phys. **741**, 51 (2008).
[8] C. Csáki, N. Kaloper, and J. Terning, Phys. Rev. Lett. **88**, 161302 (2002).
[9] C. L. Carilli and G. B. Taylor, Annu. Rev. Astron. Astrophys. **40**, 319 (2002).
[10] B. E. Schaefer, Astrophys. J. **660**, 16 (2007).
[11] S. D. Bloom, AIP Conf. Proc. **921**, 299 (2007).
[12] G. Z. Xie, Y. H. Zhang, and J. H. Fan, Astrophys. J. **477**, 114 (1997).
[13] A. T. Steffen *et al.*, Astron. J. **131**, 2826 (2006).
[14] G. Bao *et al.*, Astrophys. J. **487**, 142 (1997).